# ICLAS of HDO between 13,020 and 14,115 cm -1 — Source link ↗

Olga V. Naumenko, Olga V. Naumenko, Serge Béguier, O.M. Leshchishina ...+2 more authors

Institutions: Joseph Fourier University, Russian Academy of Sciences

Related papers:

- Intracavity laser absorption spectroscopy of HDO between 11 645 and 12 330 cm−1

- Intracavity laser absorption spectroscopy of D2O between 11 400 and 11 900 cm 1

- The absorption spectrum of water between 13 540 and 14 070 cm−1: ICLAS detection of weak lines and a complete line list

- D216O: ICLAS between 13 600 and 14 020 cm−1 and normal mode labeling of the vibrational states

- High sensitivity ICLAS of H218O in the region of the second decade (11520–12810cm−1)

# ICLAS of HDO between 13020 and 14115 cm-1

O. V. Naumenko, Serge Béguier, Olga Leshchishina, Alain Campargue

# ICLAS of HDO between 13020 and 14115 cm⁻¹

O. V. Naumenko\*[#], S. Béguier\*, O.M. Leshchishina \*[#] and A. Campargue\*[1]

*\* Laboratoire de Spectrométrie Physique (associated with CNRS, UMR 5588),
Université Joseph Fourier de Grenoble, B.P. 87, 38402 Saint-Martin-d'Hères, Cedex, France
[#] Institute of Atmospheric Optics, Russian Academy of Sciences, Siberian Branch, Tomsk,
634055, Akademicheskii av.,1, Russia*

Keywords*: water, deuterated water, HDO, Intracavity Laser Absorption Spectroscopy,
ICLAS, Rovibrational assignment, vibrational labeling, HITRAN*

*Running head: ICLAS of HDO near 13800 cm⁻¹*

---

[1]       Corresponding author: Alain.Campargue@ujf-grenoble.fr

**Abstract**

The high resolution absorption spectrum of monodeuterated water, HDO, has been recorded by Intracavity Laser Absorption Spectroscopy (ICLAS) in the 13020-14115 cm$^{-1}$ region dominated by the $4\nu_3$ band. The achieved noise equivalent absorption ($\alpha_{min} \sim 10^{-9}$ cm$^{-1}$) allowed detecting transitions with line strengths as small as $2 \times 10^{-27}$ cm/molecule which is about 10 times lower than the smallest line intensities previously detected in the region.

The rovibrational assignment of the spectrum was based on the results of the variational calculations of Schwenke and Partridge (SP) as well as recent calculations using a new potential energy surface performed by Voronin, Tolchenov and Tennyson (VTT). 2157 transitions involving 21 upper vibrational states were assigned to HD$^{16}$O while only four bands were previously reported in the region. A set of 157 new energy levels could be derived. It includes rotational levels of several highly excited bending states, in particular the (0 11 0) pure bending state. For some states like the (103) and (023) Fermi dyad, effective Hamiltonian modelling was needed to establish the vibrational assignments of some rotational levels. VTT calculations were found to significantly improve SP results, the *rms* deviation of the calculated and observed energies being decreased from 0.23 to 0.06 cm$^{-1}$.

Finally, 79 transitions of the $4\nu_3$ band of the HD$^{18}$O isotopologue were assigned, leading to the derivation of 48 levels which are the most excited energy levels reported so far for this isotopologue

# I. INTRODUCTION

The stronger absorption lines of $H_2^{16}O$ and its isotopologues are well known from the microwave to the visible regions. However, weak transitions involving highly excited energy levels are still not properly accounted both experimentally and theoretically. This contribution is aimed at recording and assigning the weak $HD^{16}O$ transitions between 13020 and 14115 $cm^{-1}$ which includes the strong $\Delta V_{OH}=4$ stretching overtone centred at 13853.6 $cm^{-1}$. The strongest HDO lines of the region have intensities on the order of $10^{-23}$ cm/molecule which makes difficult the detection of transitions with intensity at the $10^{-26}$ cm/molecule level. A further difficulty is due to the inevitable superposition with strong absorption lines of similar intensity due to the main isotopologue and with weaker lines of the $D_2O$ species.

Ten years ago, we obtained the first HDO spectra in the region by Intracavity Laser Absorption Spectroscopy (ICLAS) using dye lasers as ICLAS spectrometers [1, 2]. More recently, the wide 11500–23000 $cm^{-1}$ region was studied by Fourier Transform Spectroscopy (FTS) associated with a 600 m absorption path length [3]. A similar sensitivity (about $2\times10^{-26}$ cm/molecule for pure HDO) was achieved in the two studies. The present work is intended to achieve a higher sensitivity by using a titanium sapphire laser instead of dye lasers for ICLAS. It will allow *(i)* completing the previous measurements by new observations of weak transitions beyond the FTS sensitivity *(ii)* replacing our first ICLAS line lists [1, 2] by a more complete dataset where the calibration problem (on the order of 0.01 $cm^{-1}$) evidenced [3] for the 13100-13500 $cm^{-1}$ region [2] will be corrected. The increased sensitivity of the new recordings is demonstrated on Fig. 1, where the new ICLAS observations are superimposed to the FTS [3] spectrum.

The rovibrational assignment was performed on the basis of Schwenke and Partridge (SP) predictions [4,5] and recent variational calculations by Voronin, Tolchenov and Tennyson (VTT) [6] using a new $HD^{16}O$ potential energy surface (PES) [7]. SP line lists of $HD^{16}O$ and $HD^{18}O$ can be downloaded from the IAO database [9].

Note that the same ICLAS:Ti-Sa set up was recently used to investigate the $H_2^{16}O$ [10] and $D_2O$ [11, 12] spectra in the same region. The obtained line lists will be used in the assignment process to discriminate the $D_2O$ and $H_2^{16}O$ transitions superimposed with the HDO lines. Finally, it is worth mentioning that the analysis of the ICLAS spectrum of HDO has been reported recently [13] in the nearby 12145-13160 $cm^{-1}$ region corresponding to much weaker HDO absorption lines.

## II. EXPERIMENTAL DETAILS

The spectra were recorded with the ICLAS spectrometer based on a Ti: Sapphire laser described in Refs. [10, 14, 15]. The occupation ratio of the laser cavity by the 65 cm long absorption cell was 42 %. The spectra were recorded with a generation time of 190 $\mu$s corresponding to an equivalent absorption path length of about 24 km. The intracavity sample cell was filled at a typical pressure of 18.4 hPa. Deuterated water was obtained by mixing liquid $H_2O$ and $D_2O$. Two $D_2O:H_2O$ mixing ratios were used for the recordings: below 13550 $cm^{-1}$, $D_2O$ and $H_2O$ were mixed in equal quantities leading to a 1:2:1 proportion for $H_2O:HDO:D_2O$ in the gas phase. Above 13550 $cm^{-1}$, a higher deuterium enrichment was used in order to decrease the absorption of the strong $\Delta V_{OH}=4$ stretching overtone of $H_2^{16}O$ which may obscure many HDO lines. The $D_2O$ absorption being very weak [11, 12], we used a 5:1 mixing ratio for $D_2O$ and $H_2O$ in the liquid phase. It led to a factor of 10 for the $HDO:H_2O$ relative concentration in the gas phase which helped to detect very weak HDO lines. The contribution of the intracavity air (oxygen A band below 13160 $cm^{-1}$ and water vapor) was minimized by flowing continuously dry nitrogen in the box containing the Ti:Sa laser.

The ICLAS spectrum was obtained by successive recordings of 12 $cm^{-1}$ wide spectral sections with the help of a 3754 diodes silicon array. The 13020-14115 $cm^{-1}$ region was covered by a total of 124 spectral snapshots overlapping by about 3 $cm^{-1}$ on each side. Each of these individual spectra was calibrated independently using reference line positions. As far as possible we adopted the FTS line positions reported in Ref. [3] as reference lines. In some spectral sections, this line list was too sparse and we used the $H_2^{16}O$ line positions of Ref. [16]. Finally, in the lower energy region below 13160 $cm^{-1}$, $H_2^{16}O$ and HDO lines are very weak and we took advantage of the transitions of the oxygen A band (due to residual oxygen inside the Ti:Sa cavity) to calibrate the spectra. The lack of precise reference lines may have led to errors up to 0.010 $cm^{-1}$ in some very limited cases but we estimate that the accuracy of the wavenumber calibration is on the order of 0.005 $cm^{-1}$ as it will be confirmed below by the uncertainty obtained for the energy levels retrieved from several transitions.

The line positions and relative line intensities were determined by using an interactive least squares multi-lines fitting program assuming a Voigt profile for each line. The position and integrated absorbance of each line were derived from the multiline fitting procedure. The analysis was made difficult by the numerous strong absorption lines saturated in our spectra. As our measurements were mostly devoted to weak lines, some strong lines with distorted intensity and centre were excluded from the line lists below 13750 $cm^{-1}$. Above this value, some transitions have intensities on the order of $10^{-23}$ cm/molecule *ie* more than 1000 times

larger than our detectivity threshold. In such conditions, we preferred to limit the line profile fittings to spectral intervals showing newly observed HDO transitions.

The difficulty to estimate accurately the HDO partial pressure in the ICLAS cell added to the uncertainty on the absolute line intensity values. In principle, the HDO concentration should be determined for each 12 cm$^{-1}$ wide spectrum as deuterated water is renewed for each recording and the $H_2O$:HDO:$D_2O$ proportion may evolve from one recording to the next. We then found more reliable to normalize the relative intensity values retrieved from each elementary spectrum, against the intensity values either measured by FTS [3] or calculated by Schwenke and Partridge [4]. Such normalization is justified by the good agreement observed up to the visible range between SP and FTS [3] intensity values. In consequence of the difficult and laborious process followed in the line list construction, the obtained intensity values should be used with caution. We cannot rule out errors on the order of 50 % in the case of strongly blended lines with intensities smaller than $10^{-26}$ cm/molecule. Nevertheless, the obtained intensity information was crucial in the assignment process (see below).

The most complete line list was obtained by gathering the line lists associated with the 124 individual spectra. As several recordings of the same spectral window were often performed and because of overlapping regions, the corresponding line parameters were automatically averaged. Two lines were considered as identical when both the difference of their positions was less than 0.008 cm$^{-1}$ and their absolute intensities differed by at most a factor of 2. The obtained global line list was further checked and cleaned from $D_2O$ and $H_2^{16}O$ lines on the basis of the line list attached to Refs. [10, 16] and Refs. [12, 13], respectively. It led to the list of 1877 lines which is the one considered below for the rovibrational analysis. This line list includes about 1000 HD$^{16}$O lines which were not detected by FTS (see Fig. 1). The weakest lines detected have intensity on the order of $2 \times 10^{-27}$ cm/molecule *ie* about one order of magnitude lower than the FTS measurements [3]. As the ICLAS intensity values of the strongest lines were frequently distorted due saturation effects, we have transferred the FTS [3] intensities values for the 234 lines with intensities larger than $2.0 \times 10^{-25}$ cm/molecule (as indicated in the Supplementary Material). Figs. 2 and 3 illustrate the achieved sensitivity of the recordings in two selected spectral sections.

## III. SPECTRUM ANALYSIS

The 1877 absorption lines of our list were assigned to 21 upper vibrational states of HD$^{16}$O and to the (004) state of HD$^{18}$O. Taking into account multiple assignments, they correspond to 2157 transitions. The identification line list including observed positions and

intensities followed by VTT and SP calculated values and rovibrational assignments is attached to this paper as Supplementary Material.

### HD$^{16}$O isotopologue

#### a) Energy levels derivation

A number of new high $J$ and $K_a$ energy levels has been derived for the three strongest bands while only small $J$ and $K_a$ transitions have been assigned to three new very weak absorption bands: (510)-(000), (401)-(000) and (132)-(000) at 14147.50, 14024.58 and 13960.08 cm$^{-1}$, respectively. The summary of the obtained information is presented in Table 1. As transitions reaching the [000] rotational level were not detected, the pure vibrational energies of the (510), (401) and (132) vibrational HD$^{16}$O states were estimated from an extrapolation at $K_a$ =0 of the (Obs.- Calc.) differences between the derived and calculated energy levels.

Overall, 571 rovibrational energy levels have been derived, 157 of them being reported for the first time. Fig. 4 shows the (Obs.-Calc.) deviations of the HD$^{16}$O energy levels plotted versus $J + K_a$ /$J$ for SP [5] and VTT [6, 7] calculations. The recent VTT calculations are clearly more accurate: the *rms* deviations are 0.06 and 0.23 cm$^{-1}$ for VTT and SP, respectively, while the largest deviations reach a value of 0.80 cm$^{-1}$ for SP to be compared to 0.22 cm$^{-1}$ for VTT. As an example, the deviations for the (004) and (401) energy levels are highlighted with different symbols on Fig. 4. The spectra comparisons included in Figs. 2 and 3 show the very good agreement between the observed and VTT predicted spectra.

We have performed a detailed comparison of the energy levels of the (004), (023) and (103) vibrational states in common with the FTS set of Ref. [3]. The obtained values are comparable in terms of accuracy for most of the levels but the accuracy of the high $J$ and $K_a$ energy levels corresponding to the weakest transitions in the FTS line list is generally improved by the present measurements. The complete set of the derived HD$^{16}$O energy levels is attached as Supplementary Material.

#### b) High-order resonances and rovibrational labelling

The HDO molecule is known to undergo strong centrifugal distortion effects connected with the large amplitude excitation of the $\nu_2$ bending vibration (see [3,17] for example). It induces high-order resonance interactions with highly excited bending states resulting in intensity transfers which make observable the corresponding transitions. The high sensitivity of the present recordings allowed detecting very weak transitions reaching some of these "dark" states. Some transitions with (151), (052), (071), (081), (180), (190), and (0 11 0)

(SP labelling) upper states could be identified. As the SP vibrational labels are sometimes erroneous or ambiguous and as no labels are provided by VTT calculations [7], these labellings were checked and sometimes corrected on the basis of effective Hamiltonian (EH) calculations. The labellings of the levels of the (103) and (023) dyad were the most problematic. Using the EH approach, we could obtain an approximate global EH fitting of these two interacting states with an *rms* value of 0.08 cm^{-1}. The effective Hamiltonian used in the calculation was based on the Pade-Borel approximants [8]. The maximal normal mode contribution to the wave function provided unambiguous rovibrational labelling for most of the levels. Some of the SP labels had to be corrected as a different normal mode state was clearly dominant in the expansion of the EH wavefunction. The mixing coefficients of the wavefunctions of the (103) and (023) dyad are presented in the Supplementary Material, as they may be useful for labelling the new rovibrational energy levels in future studies of these states.

The labelling of the highly excited bending vibrational states is very difficult, too. These states are involved in series of resonance interactions which may lead to large shifts (up to several tens of cm^{-1}) in their rotational energy levels compared to the unperturbed values. For this reason, a number of EH calculations were performed to confirm that the series of the presently observed $K_a$ =1 energy levels with $J$ =1- 4 belong to the (0 11 0) pure bending state (see Table 2 and Supplementary Material). The corresponding transitions borrow their intensities from much stronger lines of the $4\nu_3$ band. The vibrational labelling of this (0 11 0) state predicted [7] at 13326.84 cm^{-1} has been confirmed by the results of Ref. [3]. However, the $K_a$ =1 energy levels are by more than 500 cm^{-1} higher than those with $K_a$ =0, that hindered the straightforward assignment even in case of the [111] and [110] rotational levels. The upper states differing by one bending excitation, the (004)-(0 11 0) interaction shows a great similarity with the previously analysed (014)-(0 12 0) resonance interaction [3, 10]. A careful comparison of the $K_a$ =1 rotational sublevels derived for the (0 12 0) state in Refs. [3, 17] confirmed our labelling of the transitions reaching the [110], [211] and [414] sublevels of the (0 11 0) state (see Table 2). These considerations also made it clear that the (052) vibrational labelling given in Refs. [1, 3] for the [312], [515] and [616] levels at 13964.294, 14065.157 and 14150.219 cm^{-1}, respectively, had to be changed to (0 11 0). Our new identifications are also confirmed by the fact that all these (0 11 0) energy levels show similar (Obs.-Calc.) deviations for both VTT and SP calculations.

*c) Observed and calculated intensities*

Intensity information provides another approach to support the assignments. The comparison presented in Fig. 5 shows that the two sets of calculated intensities agree better with each other than with the experiment. It is probably a consequence of the difficulty of retrieving accurate intensity of weak line in a strong absorbing region. However, as evidenced in our previous study [4], in some specific cases connected with the resonance redistributions of the intensities, VTT results were found to match better with the experiment. This concerns for example, transitions on the (0 11 0) [312] and (0 11 0) [515] upper energy levels at 13964.294 and 14065.157 cm$^{-1}$, respectively, which interact with the (004) [312] and (004) [505] levels at 13964.824 and 14065.628 cm$^{-1}$, respectively.

We have included in Table 1, the values of ratios of the sum of the VTT and SP calculated intensities limited to the observed transitions. Important disagreements are noted for the weakest bands: compared to SP values, VTT intensities are weaker by up to a factor of 2-3 for part of the transitions the (212)-(000) band, by 25-30% for the transitions of the (401)-(000) band while the VTT intensities of the (132)-(000) band exceed by about 40-50% the SP values. The intensities of the very weak (151)–(000) and (340)-(000) bands have a clear resonance origin and also differ significantly. As these differences concern mostly the weakest observed transitions with measured intensities with large uncertainties, it is difficult to judge definitely, which calculations are more accurate.

*The 4$v_3$ band of the HD$^{18}$O isotopologue*

Seventy nine very weak transitions of the HD$^{18}$O isotopologue could be newly detected and attributed to the 4$v_3$ band, leading to the derivation of 48 energy levels of the (004) vibrational state. (The ground state energy values were taken from Ref. [18]). The relative abundance of HD$^{18}$O compared to HD$^{16}$O was estimated from the measured intensities. We obtained a value of 7.2×10$^{-3}$ indicating a significant $^{18}$O enrichment abundance compared to the $^{18}$O natural abundance (2×10$^{-3}$). The term value of the well isolated (004) state of HD$^{18}$O ($E_v$= 13814.526 cm$^{-1)}$ has been accurately fitted by using a Watson–type rotational Hamiltonian. Rotational and centrifugal distortion constants of the (004) state of HD$^{18}$O are given in Table 3. The energy levels of the (004) state of HD$^{18}$O are included in Table 4 where deviations from SP variational calculations [4, 9] are also shown.

# IV. CONCLUSION

Weak absorption lines of the $HD^{16}O$ and $HD^{18}O$ molecules have been recorded by ICLAS between 13020 and 14115 cm$^{-1}$. The observed transitions have been assigned by using the high accuracy SP [5,6,9] and VTT [6, 7] variational calculations. The obtained set of 619 rovibrational energy levels includes 157 and 48 newly reported levels for $HD^{16}O$ and $HD^{18}O$, respectively. Transitions of the very weak (510)-(000), (132)-(000) and (401)-(000) absorption bands of $HD^{16}O$ have been identified and the corresponding band origins have been accurately evaluated from the (Obs.-Calc.) extrapolation at $J= 0$ of the $K_a=0$ series of energy levels. The new results include 48 energy levels of the (004) vibrational state of the $HD^{18}O$ isotopologue at 13814.526 cm$^{-1}$ which is the most excited vibrational state reported so far for this species.

Transitions reaching the $K_a=1$ energy levels of the (0 11 0) bending state of $HD^{16}O$ at 13326.84 cm$^{-1}$ have been observed due to intensity transfers from the (004) state *via* high-order resonance interactions. The quality of the new VTT variational calculations [6,7] has been confirmed for the $HD^{16}O$ line positions (see Figs. 2 and 3). For the derived levels, the *rms* value of the (Obs.-Calc.) deviations has been decreased to 0.06 cm$^{-1}$ compared to 0.23 cm$^{-1}$ for SP results. In addition, VTT calculations provide more accurate intensities for the transitions in close resonance. Significant discrepancies between SP and VTT calculated intensities were evidenced for the weak (212)-(000), (132)-(000) and (401)-(000) bands which are mostly free of resonance interactions, but the accuracy of the experimental intensity values of the corresponding very weak lines is not sufficient to decide which of the two calculations is more accurate.

The most complete and accurate identification list in the considered region will be generated by combining the present ICLAS results with the FTS data of Ref. [3] for the stronger transitions. It will significantly improve and replace the previous ICLAS measurements [2]. The newly reported transitions will be included into the exhaustive $HD^{16}O$ and $HD^{18}O$ datasets used by the IUPAC task group [19] to determine and evaluate a consistent set of energy levels for these two isotopologues.

## REFERENCES

1. Naumenko O, Bertseva E, Campargue A. The 4VOH Absorption Spectrum of HDO. J Mol. Spectrosc 1999;197:122-132.

2. Naumenko O, Bertseva E, Campargue A, Schwenke D. Experimental and ab inition studies of the HDO absorption spectrum in the 13 165 – 13 500 cm$^{-1}$ spectral region. J. Mol. Spectrosc. 2000;201:297-309.

3. Voronin BA, Naumenko OV, Carleer M, Coheur PF, Fally S, Jenouvrier A, Tolchenov RN, Vandaele AC, Tennyson J. HDO absorption spectrum above 11 500 cm$^{-1}$: Assignment and dynamics. J Mol Spectrosc 2007;244:87-101.

4. Partridge H, Schwenke DW. The determination of an accurate isotope dependent potential energy surface for water from extensive ab initio calculations and experimental data. J Chem Phys. 1997;106:4618-39.

5. Schwenke DW, Partridge H. Convergence testing of the analytic representation of an ab initio dipole moment function for water: Improved fitting yields improved intensities. J Chem Phys. 2000;113:6592-7.

6. Yurchenko SN, Voronin BA, Tolchenov RN, Doss N, Naumenko OV, Thiel W, Tennyson J, Potential energy surface of HDO up to 25000 cm$^{-1}$. J Chem Phys 2008;128:044312-12.

7. B.A. Voronin, J. Tennyson, R.N. Tolchenov, A.A. Lugovskoy, and S.N. Yurchenko, to be published.

8 Flaud JM, Camy-Peyret C, Bykov A, Naumenko Petrova O, Scherbakov A, Sinitsa LN. The High-Resolution Spectrum of Water Vapor between 11600 and 12750 cm$^{-1}$ J Mol Spectrosc 1997;183:300-9.

9. http://spectra.iao.ru

10. Campargue A, Mikhailenko SN, Liu AW. ICLAS of water in the 770 nm transparency window (12746-13558 cm$^{-1}$. Comparison with FTS databases. JQSRT 2008;109:2832-45.

11 Naumenko OV, Leshchishina OM, Béguier S, Campargue A. *Intracavity Laser Absorption Spectroscopy of D$_2$O between 12850 and 13380 cm$^{-1}$*. J Mol Spectrosc 2008;252:52-59.

12 Campargue A, Leshchishina OM, Naumenko OV. D$_2$$^{16}$O: ICLAS between 13600 and 14020 cm$^{-1}$ and normal mode labeling of the vibrational states J Mol Spectrosc 2009;254:1-9.

13 Naumenko OV, Voronin BA, Mazzotti F, Tennyson J, Campargue A. Intracavity Laser Absorption Spectroscopy of HDO between 12145 and 13160 cm$^{-1}$. *J Mol Spectrosc* 2008;248:122-133.

14 Kachanov A, Charvat A, Stoeckel F. Intracavity laser spectroscopy with vibronic solid state lasers: I. Spectro-temporal transient behaviour of a Ti:Sapphire laser. J Opt Soc Am B 1994;11:2412-21.

15 Campargue A, Stoeckel F, Chenevier M. High sensitive intracavity laser spectroscopy: Application to the study of overtone transitions in the visible range. Spectrochimica Acta Reviews 1990;13:69-88.

16 Tolchenov R, Tennyson J. Water line parameters from refitted spectra constrained by empirical upper state levels: Study of the 9500 – 14 500 cm$^{-1}$ region. JQSRT 2008;109:559-68.

17. Naumenko OV, Campargue A. High-Order Resonance Interactions in HDO: Analysis of the Absorption Spectrum in the 14 980–15 350 cm$^{-1}$ Spectral Region *J. Mol. Spectrosc.* 2000;199:59–72.

18. Mikhailenko SN, Tashkun SA, Putilova TA, Starikova EN, Daumont L, Jenouvrier A, Fally S, Carleer M, Hermans C, Vandaele AC Critical evaluation of measured rotation–vibration transitions and an experimental dataset of energy levels of HD$^{18}$O. JQSRT (2009);110:573-596.

19. Tennyson J, Bernath PF, Brown LR, Campargue A, Carleer MR, Csaszar AG, Gamache RR, Hodges JT, Jenouvrier A, Naumenko OV, Polyansky OL, Rothman LS, Toth RA, Vandaele AC, Zobov NF, Daumont L, Furtenbacher T, Gordon IF, Mikhailenko SN, Shirin SV. IUPAC critical evaluation of the rotational-vibrational spectra of water vapor. Part II. Energy levels and transition wavenumbers for HD$^{16}$O and HD$^{18}$O. to be submitted.

**Figure Captions**

**Fig. 1.**
Overview comparison of the HDO spectrum in the 13020-14115 $cm^{-1}$ region. The transitions newly measured by ICLAS are superimposed to the previous FTS measurements of Ref. [3].

**Fig. 2.**
The spectrum of deuterated water near 13225 $cm^{-1}$:
      (a) FTS measurement of Ref. [3].
      (b) ICLAS spectrum recorded at a total pressure of about 18 hPa with an equivalent absorption pathlength of 24 km.
      (c) HDO line list retrieved from the ICLAS spectrum
      (d) VTT predictions of Refs. [6,7].

**Fig. 3.**
The spectrum of deuterated water near 13450 $cm^{-1}$:
      (a) FTS measurement of Ref. [3]
      (b) ICLAS spectrum recorded at a total pressure of about 18 hPa with an equivalent absorption pathlength of 24 km. A few $H_2O$ transitions are marked with "H"
      (c) HDO line list retrieved from the ICLAS spectrum
      (d) VTT predictions of Refs. [6,7].

**Fig. 4.**
Differences between the observed and calculated values for the HDO energy levels determined from the ICLAS spectrum between 13020 and 14115 $cm^{-1}$ $cm^{-1}$:
      (a) variational calculations of Schwenke and Partridge [4,5],
      (b) variational calculations of Voronin, Tolchenov and Tennyson [6,7],
      As examples, the deviations corresponding to the (004) and (401) vibrational levels have been highlighted with full circles and stars, respectively.

**Fig. 5.**
Ratios of the experimental and calculated line intensities. The experimental values are compared to the intensity values calculated by Schwenke and Partridge [5] (upper panel) and Voronin, Tolchenov and Tennyson [6,7] (middle panel) while the lower panel shows the comparison between the two calculations.

Table 1. Summary of the information obtained by ICLAS in the 13020 - 14115 cm$^{-1}$ region and comparison of the experimental and calculated values of the vibrational terms.

| Band | Upper state energy (cm$^{-1}$) | | | Levels | | Transitions | Intensity ratio VTT /SP [b] |
|------|--------------|----------|-----------|-------|-----|-------------|------------------|
| | Experimental | VTT[6,7] | SP [4,5,9] | Total | New | | |
| HD$^{16}$O | | | | | | | |
| 042-000 | | 12516.4 | 12516.63 | 2 | 2 | 3 | 1.19 |
| 071-000 | | 12694.32 | 12694.53 | 1 | 1 | 1 | 5.83 |
| 500-000 | 12767.141 | 12767.15 | 12766.72 | 2 | 0 | 2 | 0.89 |
| 180-000 | | 12852.34 | 12852.95 | 2 | 1 | 2 | 2.80 |
| 311-000 | 12919.938 | 12920.00 | 12919.77 | 5 | 2 | 5 | 1.17 |
| 151-000 | | 12986.78 | 12986.67 | 7 | 6 | 13 | 1.40 |
| 420-000 | | 13108.45 | 13108.33 | 1 | 1 | 1 | 1.02 |
| 340-000 | | 13218.55 | 13218.09 | 4 | 4 | 10 | 1.73 |
| 023-000 | 13278.35 | 13278.33 | 13278.44 | 138 | 22 | 600 | 1.03 |
| 0 11 0-000 | | 13326.84 | 13327.59 | 6 | 3 | 9 | 0.50 |
| 103-000 | 13331.603 | 13331.58 | 13331.73 | 126 | 20 | 531 | 1.15 |
| 052-000 | | 13716.46 | 13716.98 | 5 | 1 | 9 | 0.83 |
| 081-000 | | 13797.37 | 13797.53 | 1 | 0 | 5 | 1.01 |
| 004-000 | 13853.628 | 13853.63 | 13853.93 | 183 | 26 | 777 | 1.01 |
| 190-000 | | | 13884.52 | 1 | 1 | 2 | 0.49 |
| 212-000 | | 13889.58 | 13890.01 | 5 | 5 | 7 | 0.73 |
| 132-000 | 13960.08 ± 0.05$^a$ | 13960.04 | 13960.20 | 18 | 18 | 19 | 1.53 |
| 401-000 | 14024.58 ± 0.05$^a$ | 14024.70 | 14024.25 | 16 | 16 | 17 | 0.75 |
| 510-000 | 14147.50 ± 0.05$^a$ | 14147.42 | 14147.51 | 29 | 25 | 44 | 1.09 |
| 033-010 | | 14563.08 | 14563.55 | 3 | 3 | 3 | 0.92 |
| 014-010 | 15166.104 | 15166.09 | 15166.52 | 16 | 0 | 18 | 1.00 |
| Total | | | | 571 | 157 | 2078 | 1.06 |
| HD$^{18}$O | | | | | | | |
| | Experimental | SP [4,5,9] | | Total | New | | |
| 004-000 | 13814.526 | 13814.75 | | 48 | 48 | 79 | |

Notes:

$^{a)}$ Vibrational energies are evaluated by extrapolation of the (Obs.-Calc.) values for the $K_a$=0 series (See text).

$^{b)}$ Ratio of the sum of the VTT and SP calculated values limited to the observed transitions

**Table 2.**
New experimental energy levels of the HD$^{16}$O molecule (in cm$^{-1}$) derived by ICLAS in the 13020 - 14115 cm$^{-1}$ region.

| $V_1V_2V_3$ | $J\ K_a\ K_c$ | $E_{obs}$ | $\delta E$ | $N$ | $\Delta$ | $V_1V_2V_3$ | $J\ K_a\ K_c$ | $E_{obs}$ | $\delta E$ | $N$ | $\Delta$ |
|---|---|---|---|---|---|---|---|---|---|---|---|
| 004 | 9 8 2 | 15260.0771 | 0.9 | 2 | -0.06 | 103 | 10 5 5 | 14462.5461 | | 1 | -0.04 |
| 004 | 9 8 1 | 15260.0771 | 0.9 | 2 | -0.06 | 103 | 10 6 4 | 14592.7552 | | 1 | -0.03 |
| 004 | 9 9 1 | 15442.4773 | | 1 | -0.06 | 103 | 11 2 10 | 14333.3574 | 2.0 | 2 | -0.08 |
| 004 | 9 9 0 | 15442.4773 | | 1 | -0.06 | 103 | 12 1 11 | 14497.6119 | 2.0 | 2 | -0.09 |
| 004 | 10 9 2 | 15593.5613 | | 1 | -0.06 | 103 | 12 2 11 | 14498.2318 | 1.5 | 2 | -0.07 |
| 004 | 10 9 1 | 15593.5613 | | 1 | -0.06 | 103 | 12 3 10 | 14632.2404 | | 1 | -0.08 |
| 004 | 11 6 6 | 15275.5358 | | 1 | -0.06 | 103 | 13 1 12 | 14674.8303 | 2.4 | 2 | -0.10 |
| 004 | 11 6 5 | 15275.7518 | 3.1 | 2 | -0.08 | 103 | 13 2 12 | 14675.1787 | 5.1 | 2 | -0.09 |
| 004 | 11 8 4 | 15578.2515 | | 1 | -0.07 | 510 | 1 1 0 | 14179.1091 | | 1 | 0.10 |
| 004 | 11 8 3 | 15578.2515 | | 1 | -0.07 | 510 | 2 0 2 | 14189.8502 | | 1 | 0.09 |
| 004 | 11 9 3 | 15759.7263 | | 1 | -0.06 | 510 | 2 1 2 | 14202.3542 | | 1 | 0.10 |
| 004 | 11 9 2 | 15759.7263 | | 1 | -0.06 | 510 | 2 2 1 | 14253.6390 | | 1 | 0.10 |
| 004 | 12 7 6 | 15599.4190 | | 1 | -0.07 | 510 | 2 2 0 | 14253.9217 | | 1 | 0.09 |
| 004 | 12 7 5 | 15599.4304 | | 1 | -0.09 | 510 | 3 1 3 | 14240.8049 | | 1 | 0.08 |
| 004 | 13 4 9 | 15482.6590 | | 1 | -0.09 | 510 | 3 1 2 | 14256.6794 | | 1 | 0.08 |
| 004 | 13 5 9 | 15540.6287 | | 1 | -0.07 | 510 | 3 2 2 | 14295.9739 | 1.0 | 2 | 0.09 |
| 004 | 13 6 8 | 15659.3855 | | 1 | -0.08 | 510 | 3 2 1 | 14297.3913 | | 1 | 0.09 |
| 004 | 14 2 12 | 15517.1961 | | 1 | -0.09 | 510 | 4 1 4 | 14291.7890 | 6.5 | 3 | 0.08 |
| 004 | 14 4 10 | 15709.2692 | | 1 | -0.08 | 510 | 4 1 3 | 14316.3560 | 7.9 | 3 | 0.06 |
| 004 | 15 2 13 | 15729.0032 | | 1 | -0.09 | 510 | 4 2 3 | 14352.1803 | | 1 | 0.10 |
| 004 | 15 3 13 | 15729.9408 | | 1 | -0.09 | 510 | 5 0 5 | 14350.8648 | 2.7 | 3 | 0.09 |
| 004 | 15 3 12 | 15856.8386 | | 1 | -0.11 | 510 | 5 1 5 | 14355.1114 | 4.2 | 2 | 0.08 |
| 004 | 16 2 15 | 15786.9051 | | 1 | -0.09 | 510 | 5 1 4 | 14391.7297 | 2.4 | 2 | 0.07 |
| 004 | 16 3 13 | 16093.5072 | | 1 | -0.12 | 510 | 5 2 4 | 14422.0116 | | 1 | 0.08 |
| 004 | 17 0 17 | 15811.7375 | | 0 | -0.12 | 510 | 5 2 3 | 14430.9417 | | 1 | 0.07 |
| 004 | 17 1 16 | 16009.9694 | | 1 | -0.12 | 510 | 5 3 2 | 14503.6046 | | 1 | 0.09 |
| 023 | 8 8 1 | 14790.2631 | | 1 | 0.00 | 510 | 6 1 6 | 14430.7707 | | 1 | 0.09 |
| 023 | 8 8 0 | 14790.2631 | | 1 | 0.00 | 510 | 6 1 5 | 14480.9057 | | 1 | 0.06 |
| 023 | 9 7 3 | 14719.7788 | | 1 | -0.04 | 510 | 6 2 5 | 14505.2432 | 3.4 | 2 | 0.07 |
| 023 | 9 7 2 | 14719.7788 | | 1 | -0.03 | 510 | 6 3 3 | 14590.0875 | | 1 | 0.10 |
| 023 | 9 8 2 | 14928.2716 | | 1 | -0.00 | 510 | 7 0 7 | 14515.9036 | | 1 | 0.06 |
| 023 | 9 8 1 | 14928.2716 | | 1 | -0.00 | 510 | 7 1 7 | 14517.5712 | | 1 | 0.11 |
| 023 | 10 7 4 | 14873.8714 | | 1 | -0.06 | 510 | 8 1 8 | 14616.7468 | | 1 | 0.06 |
| 023 | 10 7 3 | 14873.8715 | | 1 | -0.05 | 401 | 1 0 1 | 14038.8653 | | 1 | -0.10 |
| 023 | 11 3 8 | 14471.3718 | | 1 | -0.07 | 401 | 1 1 0 | 14054.9846 | | 1 | -0.11 |
| 023 | 11 4 8 | 14571.7861 | 0.3 | 2 | -0.08 | 401 | 2 0 2 | 14067.0848 | | 1 | -0.11 |
| 023 | 11 4 7 | 14587.4131 | | 1 | -0.09 | 401 | 2 1 2 | 14078.5617 | | 1 | -0.12 |
| 023 | 12 2 10 | 14583.1771 | | 1 | -0.06 | 401 | 2 1 1 | 14085.9985 | | 1 | -0.10 |
| 023 | 12 3 10 | 14590.3068 | | 1 | -0.05 | 401 | 2 2 0 | 14127.0380 | | 1 | -0.09 |
| 023 | 12 3 9 | 14711.3017 | | 1 | -0.11 | 401 | 3 0 3 | 14108.6831 | 6.2 | 2 | -0.11 |
| 023 | 12 4 9 | 14757.2802 | | 1 | -0.09 | 401 | 3 1 3 | 14117.4804 | | 1 | -0.11 |
| 023 | 12 4 8 | 14785.4010 | | 1 | -0.07 | 401 | 3 1 2 | 14132.2722 | | 1 | -0.12 |
| 023 | 13 1 12 | 14639.3631 | | 1 | -0.04 | 401 | 4 0 4 | 14162.8956 | | 1 | -0.12 |
| 023 | 13 2 12 | 14639.7103 | | 1 | -0.04 | 401 | 4 2 3 | 14226.2213 | | 1 | -0.12 |
| 023 | 13 7 6 | 15428.3897 | | 1 | -0.08 | 401 | 4 4 1 | 14400.5583 | | 1 | -0.07 |
| 023 | 14 1 13 | 14827.9004 | | 1 | -0.07 | 401 | 4 4 0 | 14400.5564 | | 1 | -0.07 |
| 023 | 14 2 13 | 14828.1089 | | 1 | -0.07 | 401 | 5 2 3 | 14306.0555 | | 1 | -0.11 |
| 023 | 16 1 16 | 15025.6589 | | 1 | -0.07 | 401 | 6 1 6 | 14309.1788 | | 1 | -0.14 |
| 103 | 8 5 4 | 14173.6345 | | 1 | -0.01 | 401 | 7 1 7 | 14397.4078 | | 1 | -0.14 |
| 103 | 8 5 3 | 14173.6862 | | 1 | -0.04 | 212 | 3 1 2 | 14002.6394 | | 1 | 0.00 |
| 103 | 8 7 2 | 14461.9044 | | 1 | -0.03 | 212 | 5 1 5 | 14102.7626 | | 1 | -0.00 |
| 103 | 8 7 1 | 14461.9044 | | 1 | -0.03 | 212 | 5 2 3 | 14189.1335 | 2.2 | 2 | -0.00 |
| 103 | 8 8 1 | 14638.4452 | | 1 | -0.01 | 212 | 6 0 6 | 14177.8856 | | 1 | 0.00 |
| 103 | 8 8 0 | 14638.4452 | | 1 | -0.01 | 212 | 6 1 5 | 14236.9644 | | 1 | -0.01 |
| 103 | 9 6 4 | 14442.1921 | | 1 | -0.01 | 132 | 2 2 0 | 14083.3658 | | 1 | 0.05 |
| 103 | 9 6 3 | 14442.1623 | | 1 | -0.05 | 132 | 3 0 3 | 14049.7654 | | 1 | 0.05 |
| 103 | 9 7 3 | 14596.4473 | | 1 | -0.03 | 132 | 3 1 3 | 14061.5854 | | 1 | 0.06 |
| 103 | 9 7 2 | 14596.4468 | | 1 | -0.03 | 132 | 3 1 2 | 14081.7816 | | 1 | 0.04 |
| 103 | 10 4 7 | 14351.9799 | | 1 | -0.03 | 132 | 3 2 2 | 14128.4462 | | 1 | 0.04 |
| 103 | 10 4 6 | 14360.7014 | | 1 | -0.04 | 132 | 3 3 1 | 14227.6642 | | 1 | 0.07 |

**Table 2** (*continued*)

| $V_1V_2V_3$ | $J\,K_a\,K_c$ | $E_{obs}$ | $\delta E$ | $N$ | $\Delta$ | $V_1V_2V_3$ | $J\,K_a\,K_c$ | $E_{obs}$ | $\delta E$ | $N$ | $\Delta$ |
|---|---|---|---|---|---|---|---|---|---|---|---|
| 1 3 2 | 3 3 0 | 14227.7112 | | 1 | 0.05 | 311 | 9 3 6 | 13748.1040 | | 1 | -0.14 |
| 1 3 2 | 4 0 4 | 14106.0500 | | 1 | 0.06 | 151 | 5 5 1 | 13911.5362 | | 1 | -0.02 |
| 1 3 2 | 4 1 4 | 14115.1107 | | 1 | 0.03 | 151 | 5 5 0 | 13911.5362 | | 1 | -0.02 |
| 1 3 2 | 4 1 3 | 14148.7454 | | 1 | 0.04 | 151 | 6 3 3 | 13656.3406 | 1.3 | 4 | 0.07 |
| 1 3 2 | 4 2 2 | 14195.6746 | | 1 | 0.05 | 151 | 6 5 2 | 14004.4412 | | 1 | -0.04 |
| 1 3 2 | 4 3 2 | 14289.2399 | | 1 | 0.02 | 151 | 6 5 1 | 14004.4400 | | 1 | -0.05 |
| 1 3 2 | 5 0 5 | 14175.7449 | | 1 | 0.03 | 151 | 8 5 4 | 14236.6337 | | 1 | -0.11 |
| 1 3 2 | 5 1 5 | 14181.4420 | | 1 | 0.05 | 033 | 1 0 1 | 14578.7741 | | 1 | -0.05 |
| 1 3 2 | 6 0 6 | 14256.8951 | | 1 | 0.02 | 033 | 5 1 5 | 14783.4696 | | 1 | -0.08 |
| 1 3 2 | 6 1 6 | 14260.3228 | | 1 | 0.02 | 033 | 7 0 7 | 14951.7428 | | 1 | -0.10 |
| 1 3 2 | 7 0 7 | 14349.8498 | | 1 | 0.01 | 340 | 6 3 3 | 13774.8097 | 0.3 | 2 | 0.12 |
| 1 3 2 | 8 3 6 | 14693.4852 | 5.6 | 3 | -0.01 | 340 | 7 3 5 | 13878.9211 | 1.3 | 3 | 0.08 |
| 0 5 2 | 4 2 3 | 14028.8495 | | 1 | -0.07 | 340 | 9 1 8 | 14037.0435 | 2.8 | 3 | 0.00 |
| 0 11 0 | 1 1 0 | 13875.9014 | | 1 | 0.10 | 340 | 9 3 7 | 14203.9950 | | 1 | 0.07 |
| 0 11 0 | 2 1 1 | 13911.9333 | | 1 | 0.08 | 180 | 4 2 2 | 13423.2609 | | 1 | 0.04 |
| 0 11 0 | 4 1 4 | 13995.1224 | | 1 | 0.06 | 071 | 6 2 4 | 13256.8102 | | 1 | 0.08 |
| 0 4 2 | 10 6 5 | 14177.8627 | 2.6 | 2 | -0.06 | 420 | 6 2 5 | 13478.7775 | | 1 | -0.12 |
| 0 4 2 | 11 7 5 | 14591.3399 | | 1 | -0.06 | 190 | 3 1 2 | 14254.2924 | 1.6 | 2 | -0.05 |
| 3 1 1 | 9 2 7 | 13687.2479 | | 1 | -0.06 | | | | | | |

*Notes:*

$N$ is the number of lines used for the upper level determination. $\delta E$ (in $10^{-3}$ cm$^{-1}$) denotes the corresponding statistical error defined as the *rms* value of the deviation of the levels derived through several transitions from their average value. $\Delta$ represents the deviation of the experimental level from the VTT calculated [6, 7] value in cm$^{-1}$.

**Table 3.**
Watson-type Hamiltonian parameters for the (004) vibrational state of the $HD^{18}O$ isotopologue.

| Parameter | Value, cm$^{-1}$ |
|:---:|:---:|
| $E_V$ | 13814.52616(440) |
| $A$ | 19.21035(270) |
| $B$ | 9.016468(340) |
| $C$ | 6.048101(300) |
| $\Delta_K$ | 9.620(380)E-03 |
| $\Delta_{JK}$ | 4.759(230)E-04 |
| $\Delta_{DJ}$ | 3.9420(280)E-04 |
| $\delta_K$ | 1.3586(320)E-03 |
| $\delta_J$ | 1.3739(170)E-04 |
| $H_K$ | 5.05(150)E-05 |

*Note*: The numbers in parenthesis correspond to a 68% confidence interval.

**Table 4.**
New experimental energy levels of the HD$^{18}$O molecule (in cm$^{-1}$) derived by ICLAS in the 13020 - 14115 cm$^{-1}$ region.

| $V_1V_2V_3$ | $J\ K_a\ K_c$ | $E_{obs}$ | $\delta E$ | $N$ | $\Delta$ | $V_1V_2V_3$ | $J\ K_a\ K_c$ | $E_{obs}$ | $\delta E$ | $N$ | $\Delta$ |
|---|---|---|---|---|---|---|---|---|---|---|---|
| 004 | 1 1 1 | 13839.7706 |     | 1 | -0.23 | 004 | 5 3 2 | 14148.6549 | 1.5 | 2 | -0.22 |
| 004 | 1 1 0 | 13842.7379 | 2.4 | 2 | -0.23 | 004 | 5 4 2 | 14226.1182 | 1.1 | 2 | -0.21 |
| 004 | 2 0 2 | 13859.1462 |     | 1 | -0.22 | 004 | 5 4 1 | 14226.2012 |     | 1 | -0.18 |
| 004 | 2 1 2 | 13866.9364 | 1.7 | 2 | -0.22 | 004 | 6 0 6 | 14104.2438 |     | 1 | -0.24 |
| 004 | 2 1 1 | 13875.8144 |     | 1 | -0.23 | 004 | 6 1 6 | 14104.9972 | 4.2 | 2 | -0.23 |
| 004 | 2 2 0 | 13906.8066 |     | 1 | -0.23 | 004 | 6 1 5 | 14161.9118 |     | 1 | -0.24 |
| 004 | 3 0 3 | 13902.1911 |     | 1 | -0.23 | 004 | 6 2 5 | 14172.7180 |     | 1 | -0.21 |
| 004 | 3 1 3 | 13907.3461 |     | 1 | -0.21 | 004 | 6 2 4 | 14198.3314 |     | 1 | -0.24 |
| 004 | 3 1 2 | 13925.0040 |     | 1 | -0.23 | 004 | 6 3 4 | 14238.4955 |     | 1 | -0.21 |
| 004 | 3 2 1 | 13954.0596 | 0.5 | 2 | -0.22 | 004 | 6 3 3 | 14243.2887 |     | 1 | -0.21 |
| 004 | 3 3 1 | 14009.4854 |     | 1 | -0.21 | 004 | 6 4 3 | 14317.8684 | 2.6 | 3 | -0.20 |
| 004 | 3 3 0 | 14009.5501 |     | 1 | -0.21 | 004 | 6 4 2 | 14318.1579 |     | 1 | -0.19 |
| 004 | 4 0 4 | 13957.7156 | 2.0 | 2 | -0.22 | 004 | 7 1 7 | 14195.5767 |     | 1 | -0.23 |
| 004 | 4 1 4 | 13960.6678 | 5.4 | 2 | -0.23 | 004 | 7 1 6 | 14267.0668 | 4.3 | 2 | -0.24 |
| 004 | 4 1 3 | 13989.7370 | 4.4 | 2 | -0.23 | 004 | 7 3 5 | 14344.9372 |     | 1 | -0.21 |
| 004 | 4 2 3 | 14011.1106 |     | 1 | -0.23 | 004 | 7 3 4 | 14355.4840 |     | 1 | -0.21 |
| 004 | 4 2 2 | 14018.4103 | 5.3 | 3 | -0.23 | 004 | 7 4 3 | 14426.1003 |     | 1 | -0.22 |
| 004 | 4 3 2 | 14070.5315 | 1.5 | 2 | -0.21 | 004 | 8 3 6 | 14465.8138 |     | 1 | -0.23 |
| 004 | 4 3 1 | 14070.9857 | 5.9 | 3 | -0.21 | 004 | 9 0 9 | 14412.8833 |     | 1 | -0.24 |
| 004 | 5 1 5 | 14026.6344 | 0.6 | 2 | -0.23 | 004 | 9 1 9 | 14412.9295 | 0.6 | 2 | -0.25 |
| 004 | 5 1 4 | 14069.1088 | 2.9 | 2 | -0.24 | 004 | 9 2 8 | 14513.9092 |     | 1 | -0.21 |
| 004 | 5 2 4 | 14085.0102 |     | 1 | -0.24 | 004 | 9 2 7 | 14583.7295 |     | 1 | -0.26 |
| 004 | 5 2 3 | 14099.9944 |     | 1 | -0.24 | 004 | 9 4 6 | 14685.8965 |     | 1 | -0.20 |
| 004 | 5 3 3 | 14146.9126 |     | 1 | -0.22 | 004 | 9 4 5 | 14692.3288 |     | 1 | -0.20 |

*Notes:*

$N$ is the number of lines used for the upper level determination. $\delta E$ (in 10$^{-3}$ cm$^{-1}$) denotes the corresponding statistical error defined as the *rms* value of the deviation of the levels derived through several transitions from their average value. $\Delta$ represents the deviation of the experimental level from its calculated [4,5,9] value in cm$^{-1}$.
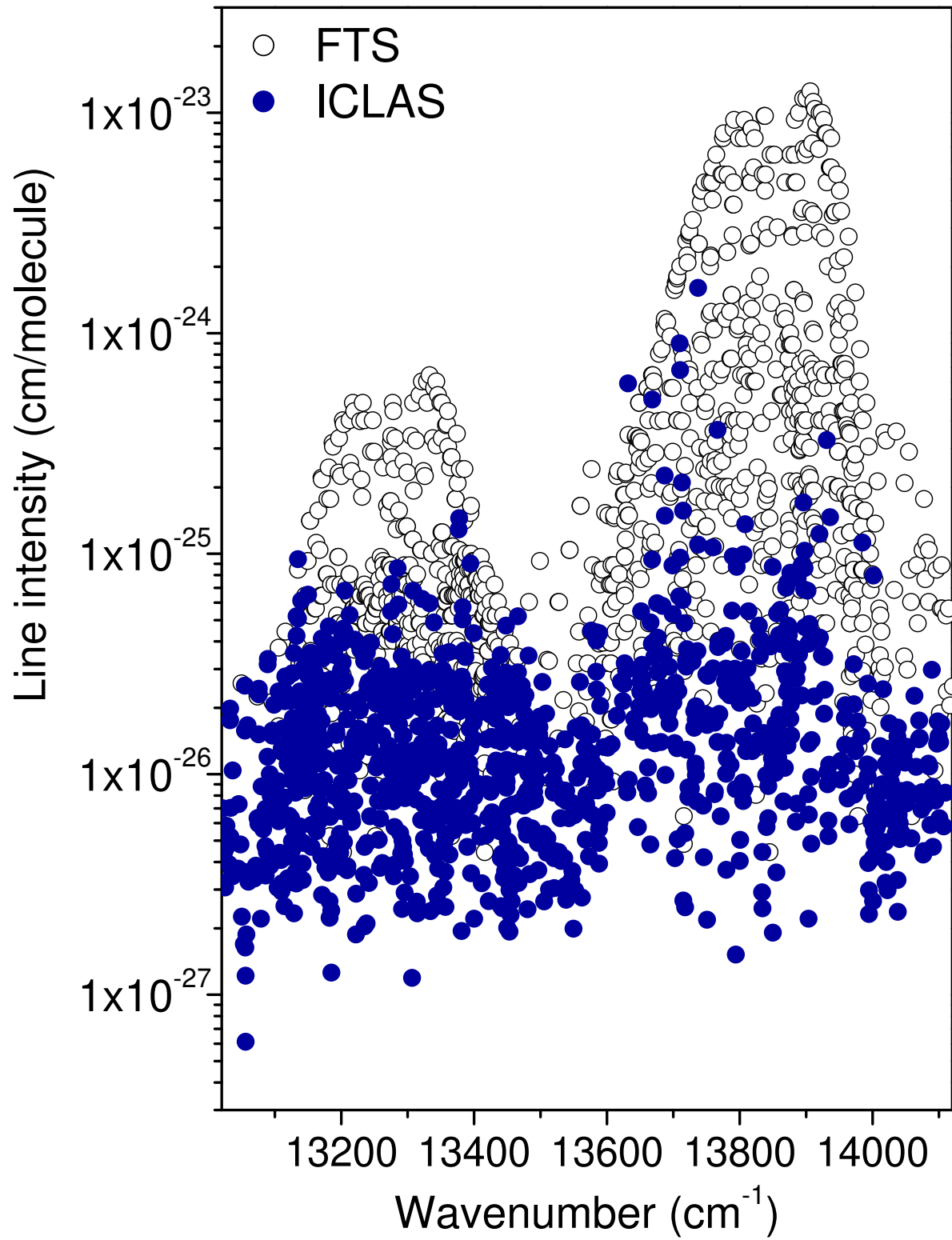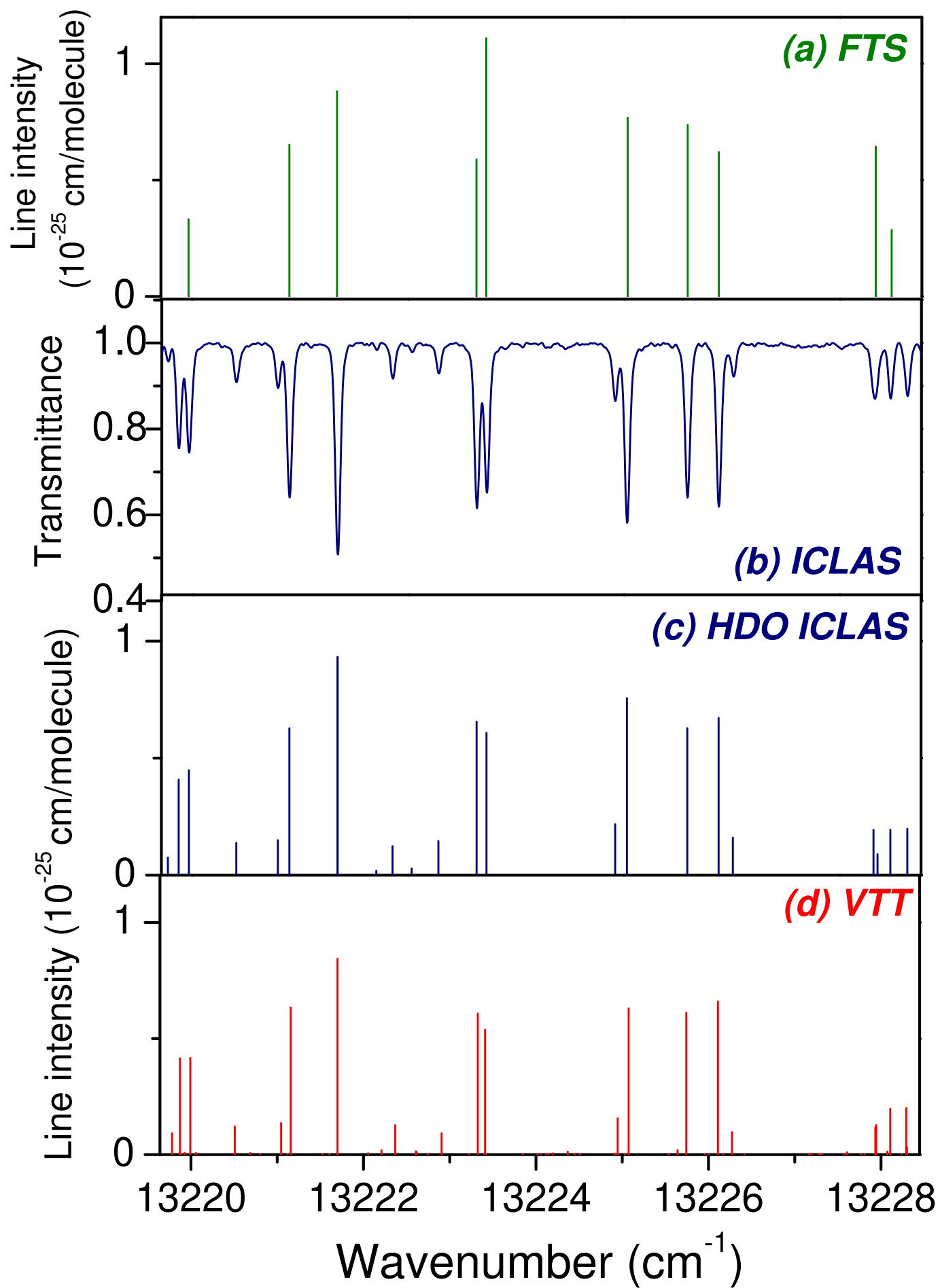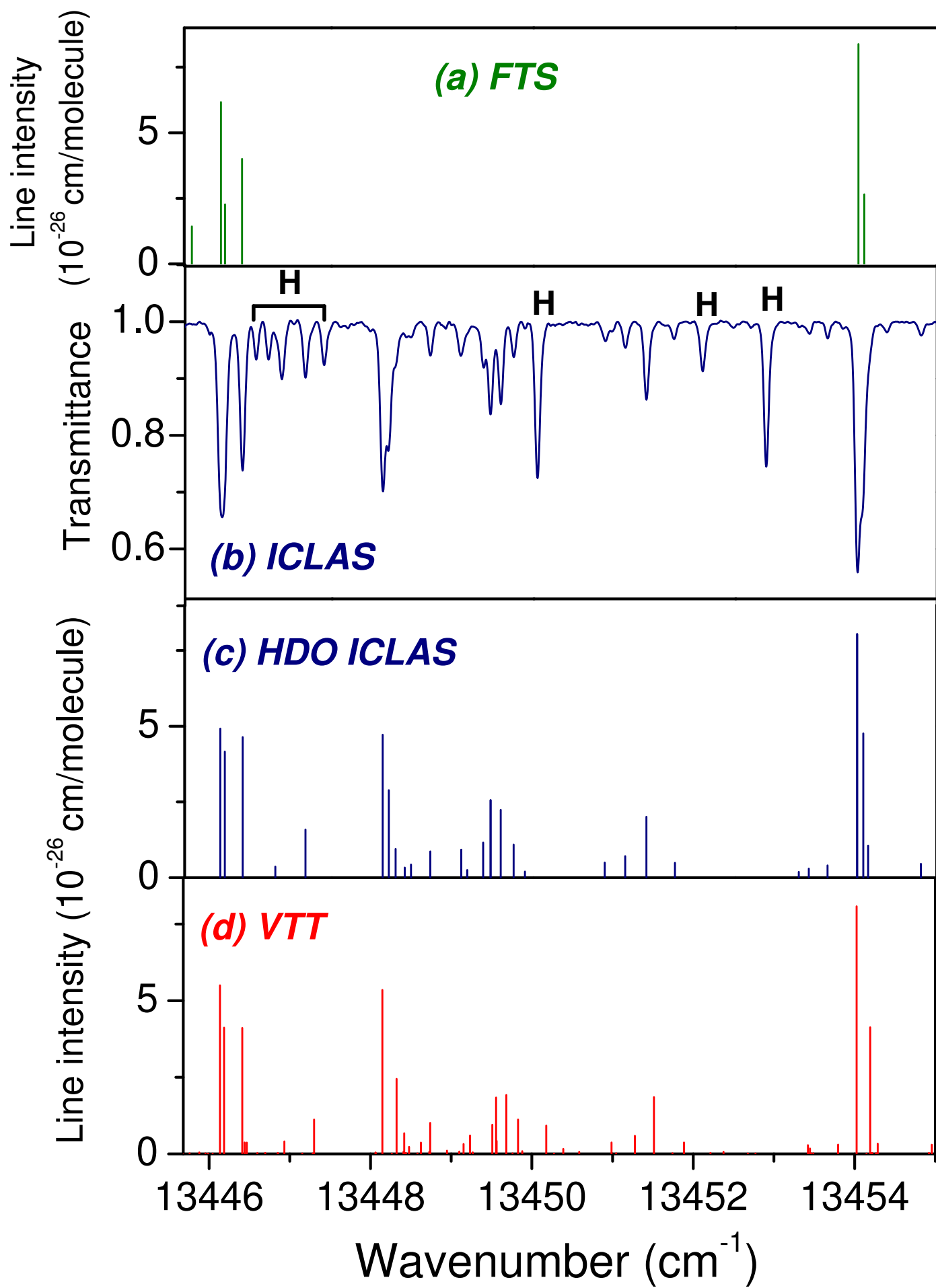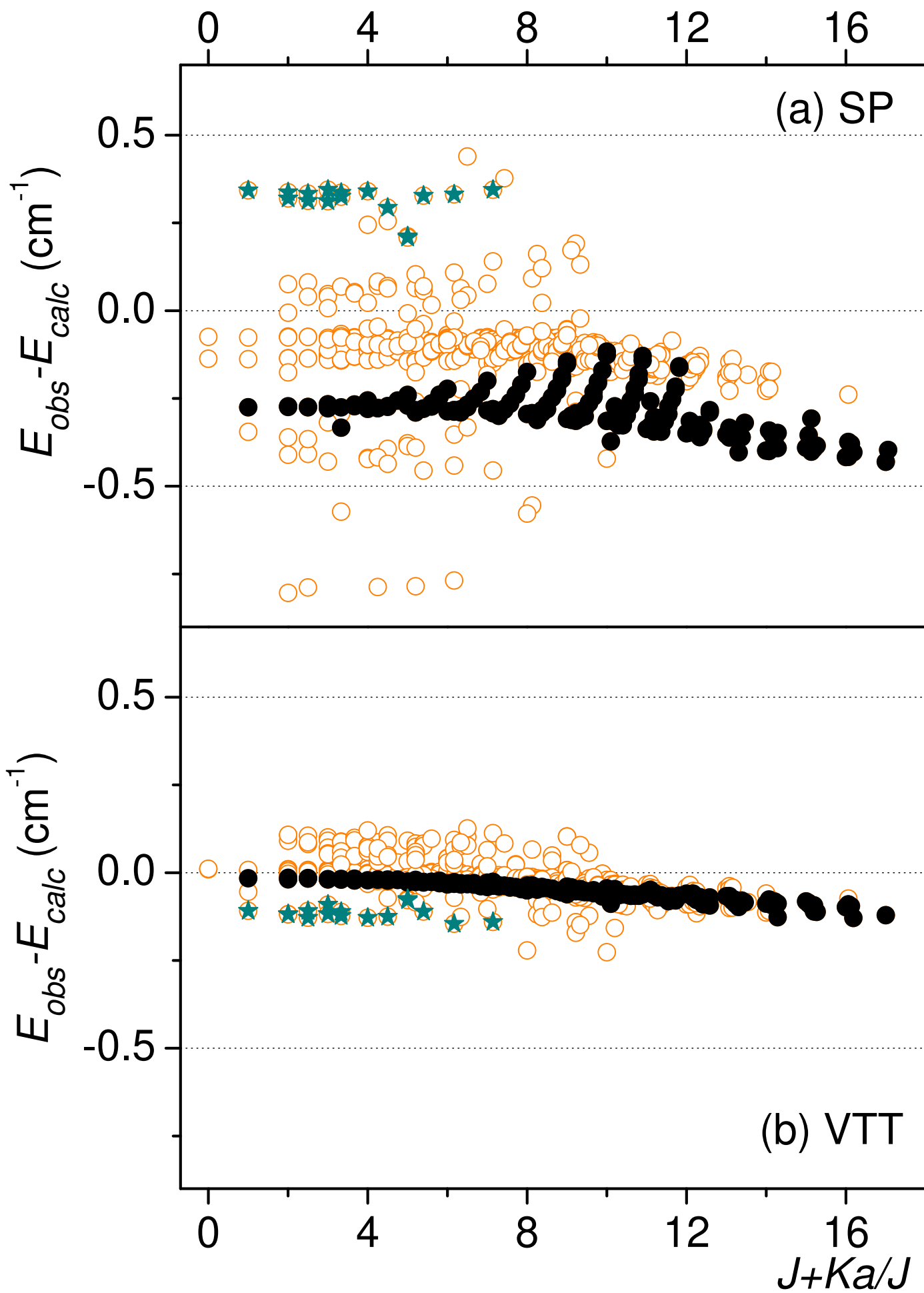
Fig. 1

Fig. 2

Fig. 3

Fig. 4

Fig. 5

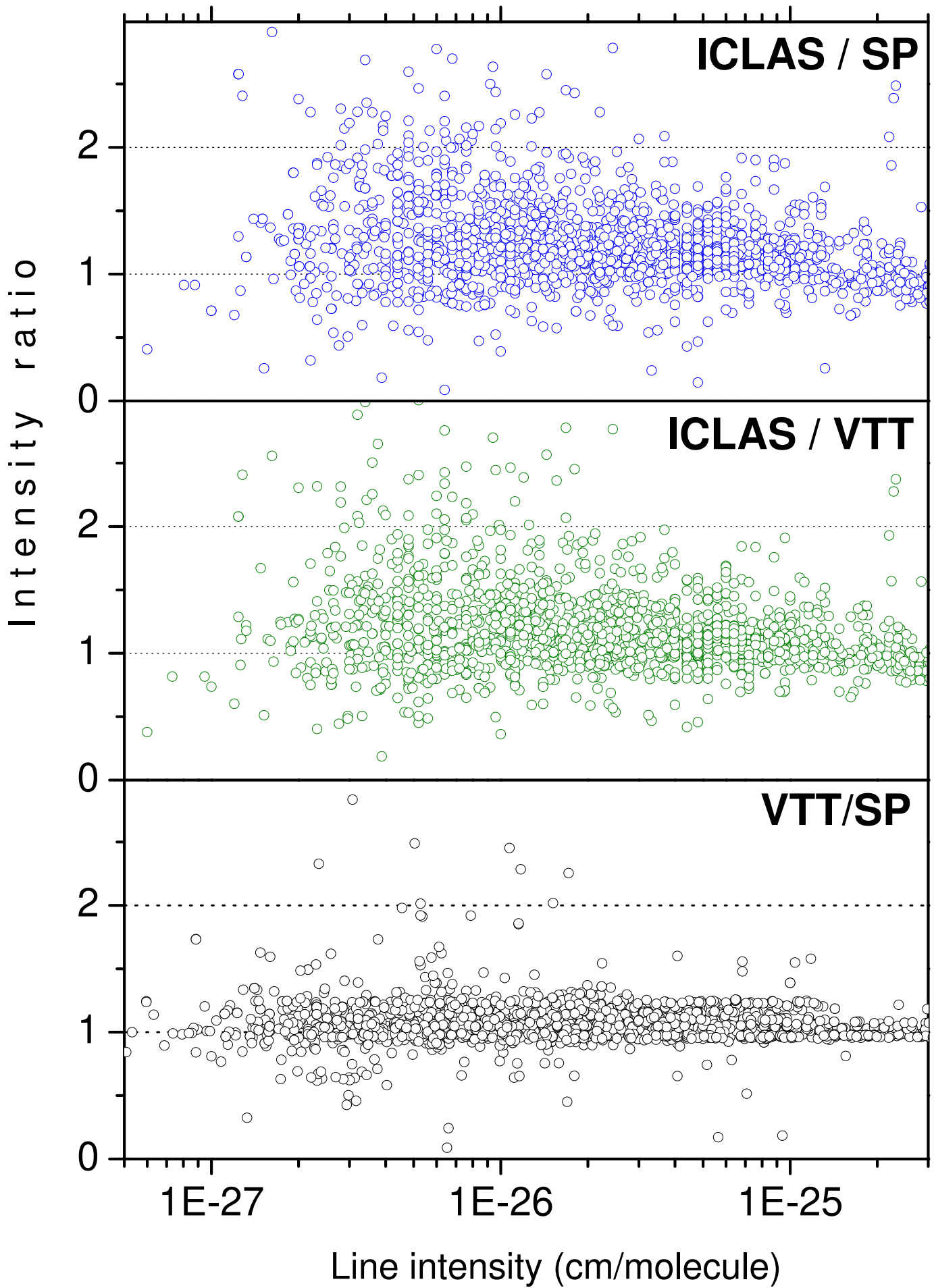**e-component, for online publication only**

**e-component, for online publication only**

**e-component, for online publication only**
**Click here to download e-component, for online publication only: SUP_MAT_MIXING**